Atmos. Chem. Phys., 9, 1–17, 2009
www.atmos-chem-phys.net/9/1/2009/

Atmospheric Chemistry and Physics

Technical Note: Measurement of the tropical UTLS composition in presence of clouds using millimetre-wave heterodyne spectroscopy

B. M. Dinelli[1], E. Castelli[1], B. Carli[2], S. Del Bianco[2], M. Gai[2], L. Santurri[2], B. P. Moyna[3], M. Oldfield[3], R. Siddans[4], D. Gerber[4], W. J. Reburn[4], B. J. Kerridge[4], and C. Keim[5,*]

[1]Istituto di Scienze dell'Atmosfera e del Clima – CNR, Bologna, Italy
[2]Istituto di Fisica Applicata "N. Carrara" – CNR, Florence, Italy
[3]"Millimetre-wave Technology Group" RAL, UK
[4]"Remote Sensing Group" RAL, UK
[5]Institut für Meteorologie und Klimaforschung, Forschungszentrum Karlsruhe, Germany
[*]now at: Laboratoire Interuniversitaire des Systèmes Atmosphériques (LISA) CNRS/ Univ. Paris 12 et 7, France

Received: 26 May 2008 – Published in Atmos. Chem. Phys. Discuss.: 23 July 2008
Revised: 16 January 2009 – Accepted: 19 January 2009 – Published:

Abstract. The MARSCHALS (Millimetre-wave Airborne Receiver for Spectroscopic CHaracterisation of Atmospheric Limb-Sounding) project has the general objectives of demonstrating the measurement capabilities of a limb viewing instrument working in the millimetre and sub-millimetre spectral regions (from 294 to 349 GHz) for the study of the Upper Troposphere – Lower Stratosphere (UTLS). MARSCHALS has flown on board the M-55 stratospheric aircraft (Geophysica) in two measurements campaigns. Here we report the results of the analysis of MARSCHALS measurements during the SCOUT-O3 campaign held in Darwin (Australia) in December 2005 obtained with MARC (Millimetre-wave Atmospheric-Retrieval Code). MARSCHALS measured vertical distributions of temperature, water vapour, ozone and nitric acid in the altitude range from 10 to 20 km in presence of clouds that obscure measurements in the middle infrared spectroscopic region. The minimum altitude at which the retrieval has been possible is determined by the high water concentration typical of the tropical region rather than the extensive cloud coverage experienced during the flight. Water has been measured from 10 km to flight altitude (∼18 km) with a 10% accuracy, ozone from 14 km to flight altitude with accuracy ranging from 10% to 60%, while the retrieval of nitric acid has been possible with an accuracy not better than 40% only from 16 km to flight altitude due to the low signal to noise ratio of its emission in the analysed spectral region. The results have been validated using measurement made in a less cloudy region by MIPAS-STR, an infrared limb-viewing instrument on board the M-55, during the same flight.

Correspondence to: B. M. Dinelli
(BM.Dinelli@isac.cnr.it)

1 Introduction

Today predictions of climate change or of trends in global air quality are a crucial issue (IPCC 2007). For this, the understanding of the radiative balance of the Upper Troposphere – Lower Stratosphere (UTLS) region and therefore of the dynamical, chemical and physical processes that control water vapour, ozone, radical constituents, aerosols, and clouds is critical. The UTLS region is roughly defined as the part of the atmosphere between 5 and 20 km. It is a transition zone between the convectively dominated and therefore unstable troposphere and the stable, stratified stratosphere. The UTLS is a highly coupled region: in it dynamics, chemistry, microphysics and radiation are fundamentally interconnected (Holton, 1995), and the strong gradients in many trace constituents of tropospheric or stratospheric origin (such as water vapour and ozone) make the study of its composition quite difficult.

In the tropics the tropopause is relatively high, with the coldest point near 17 km, and the region of the tropical atmosphere between ∼12 km and the coldest point or slightly

Published by Copernicus Publications on behalf of the European Geosciences Union.

above has characteristics intermediate between those of the troposphere and stratosphere, and is referred to as the Tropical Tropopause Layer (TTL). Thin (sometimes sub visible) cirrus clouds are observed over large areas of the TTL (Wang et al., 1996; Winker and Trepte, 1998), although their formation mechanisms and effects on the large-scale circulation and humidity are poorly known. The measurement of the composition of the TTL is one of the most challenging questions the atmospheric community is facing today. Nadir measurements performed by instruments on board of satellites (like IASI Blumstein et al., 2004; Turquety et al., 2004) can provide measurements of the TTL region with very high geographical resolution, but their vertical resolution is not high enough to give useful results. Limb sounding observations can provide the good vertical resolution needed to study the TTL region. However, limb sounding measurements observe the atmosphere with long horizontal optical paths so that the relatively thin cirrus clouds present here can attenuate significantly the atmospheric signal. So it is important to develop instruments that can avoid the attenuation of the cirrus clouds that are often present in the UTLS. Fortunately, the optical depth of cirrus clouds is not the same at all wavelengths (Warren, 1984): the relatively low extinction coefficient of ice particles at longer wavelengths (far infrared and millimetre wave spectral interval) can be exploited to measure the UTLS region also in presence of cirrus clouds (Del Bianco et al., 2007).

Retrievals of atmospheric constituents within the UTLS have been performed at millimetre wavelengths for the UTLS and at sub-millimetre wavelengths for the LS, mainly from space-borne, limb-viewing instruments. However, to date the tropical UTLS region is not properly covered by satellite instruments, since the majority of these instruments are blinded by the clouds that are very frequent in this region. To overcome this, several European Space Agency (ESA) studies (for example ACECHEM (Kerridge et al., 2004 a, b) or CAPACITY (Kelder et al., 2005) considered the use of the MASTER (Millimetre-wave Acquisition for Stratosphere-Troposphere Exchange Research) millimetre-wave heterodyne spectrometer for the study of the UTLS region. Theoretical simulations indicate that MASTER can satisfactorily meet the challenging requirements for UTLS studies (Reburn, 1998), but the full measurement capabilities of MASTER had to be demonstrated with a real instrument. The capability of the millimetre waves to measure the atmosphere has been exploited by the Microwave Limb Sounder (MLS) flown in 1991 on board of the UARS (Upper Atmosphere Research Satellite) satellite (Barath et al. 1993). However, MLS did not sound low altitudes and had a low vertical resolution and a poor sensitivity (Sandor et al, 1998; Livesey et al., 2003). MAS (Millimetre wave Atmospheric Sounder), part of the ATLAS (ATmospheric Laboratory for Application and Science) project, was flown several times in 1992–1994, but the vertical range in which it was operated was above 10 km and its vertical resolution (5–10 km) was again very low to study the UTLS region (Hartmann et al., 1996). Remarkable results have been obtained in the UTLS with the AURA/MLS instrument for O_3, CO, N_2O, H_2O, and ice cirrus clouds, (Froidevaux, 2006 and references therein), but again its vertical resolution prevented to obtain a definitive proof of the millimetre wave capabilities of measuring UTLS in presence of clouds. The ASUR (Airborne Submillimetre Radiometer) has flown on the Falcon aircraft up to about 14 km, but from this altitude it has not been possible to test its limb measurement capabilities. The Odin satellite (Murtagh et al., 2002) has better sensitivity than MLS, and measurements have been performed of the tropical relative humidity, N_2O and ice cirrus clouds (Ekström et al., 2007, 2008; Urban et al., 2005; Eriksson et al., 2007, 2008), but its channels are optimised for combined astrophysical and atmospheric requirements and its atmospheric measurements are not fully optimised for UTLS studies. A few other submillimetre radiometers, such as the JEM/SMILES (Superconducting MIllimetre-wave Limb-Emission Sounder) that is planned for the International Space Station (ISS) (Masuko et al., 2000) and others that have been deployed either on aircraft or balloon, operate in bands that are not optimised for the UTLS region.

In order to verify experimentally the measurement capabilities of MASTER, ESA has developed the MARSCHALS (Millimetre-wave Airborne Receiver for Spectroscopic CHaracterisation of Atmospheric Limb-Sounding) instrument (Oldfield et al., 2001). MARSCHALS is a heterodyne spectrometer that can be operated on board of stratospheric aircrafts or balloons. It is designed to sample the atmosphere using a limb-viewing geometry. MARSCHALS has flown on board the M-55 stratospheric aircraft (Geophysica) in two measurements campaigns.

Along with the development of the instrument, ESA has devoted a separate study to the development of a dedicated code (Millimetre-wave Atmospheric-Retrieval Code, MARC) for the analysis of its measurements (Carli et al., 2007). In this work we present the results of MARSCHALS measurements during the SCOUT-O3 campaign held in Darwin (Australia) in December 2005, obtained with MARC. The analysis aimed at the assessment of atmospheric measurements capabilities of the millimetre waves in presence of clouds and high water vapour concentration as experienced in the tropical UTLS.

2 The instrument

MARSCHALS views thermal emission from the atmospheric limb using a scanning 235 mm diameter antenna via an open aperture in the starboard side of the Geophysica aircraft. Measurement of the incoming radiation is time-shared between each of the three millimetre-wave heterodyne radiometers centred at 300, 325 and 345 GHz, where it is down-converted to an IF range of 12–24 GHz.

Table 1. MARSCHALS instrument specification.

Instrument Type	Total Power Single Sideband Radiometer
RF target bands	Band B 294 – 305.5 GHz Band C 316.5 – 325.5 GHz Band D 342.2 – 348.8 GHz
Instantaneous bandwidth	12 GHz
Spectral Resolution	200 MHz (with provision for addition of high resolution spectrometer with up to 12 GHz bandwidth)
Tsys	∼20 000 K (Bands B and C)
NET (250 ms)	2–4 K (Bands C and D) 4–6 K (Band B)
NET (8 scans)	1 K (Band C)
Sideband Rejection	>30 Db
Beam Width	0.34° HPBW (2 km at 10 km tangent height)
Beam Pointing	≪0.0025 deg. rms pointing knowledge during scan, bias excepted
Scan range	Tangent heights from −2 km to platform altitude (21 km on aircraft) in 1 km steps with +20° "space view"
Mass	330 kg
Dimensions	1.55×0.76×0.56 m

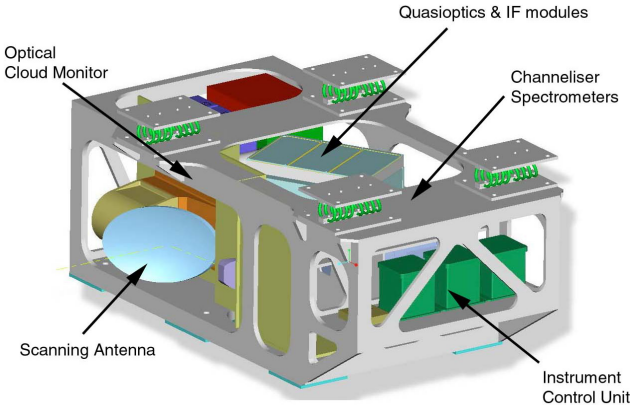

Fig. 1. MARSCHALS instrument configuration.

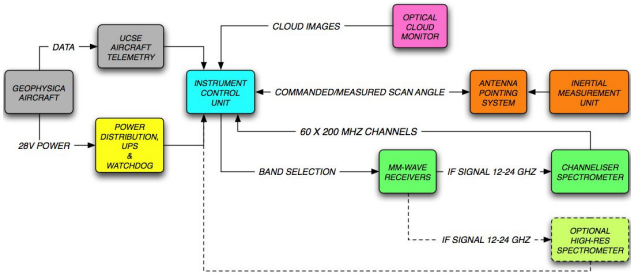

Fig. 2. Millimetre-wave receiver signal flow.

The down-converted signal from each mm-wave receiver is fed to a spectrometer. At present, channeliser (filter bank) spectrometers are used, having 60 channels each of 200 MHz bandwidth for a total instantaneous bandwidth of 12 GHz. This is adequate for measurements at the flight altitudes of the Geophysica aircraft (<21 km), however MARSCHALS has been designed for future expansion with a high resolution spectrometer, e.g. a Digital Autocorrelator or Acousto-Optic Spectrometer in the event that a higher-altitude balloon platform is employed. Each radiometer incorporates a high performance single sideband filter which passes the signal due to the target species (O_3, H_2O and CO respectively) and rejects aliased radiances by at least 30 dB.

In order to improve the antenna pointing, the antenna scan system employs a dedicated Inertial Measurement Unit (IMU); the instrument (aircraft) roll angle is measured with high precision and corrected for in the antenna control loop, resulting in an extremely stable line-of-sight.

MARSCHALS also incorporates a near-infrared Optical Cloud Monitor (OCM) to aid in assessing the impact of cirrus on mm-wave observations.

2.1 Instrument configuration

The layout of the instrument is shown in Fig. 1. The individual subsystems are mounted in an open frame designed to fit in the front bay of the M55 Geophysica airplane. The scanning antenna and OCM are located on the starboard side of the instrument. All acquisition of measurement and housekeeping data is performed by the instrument control units at the front of the instrument. A brief summary of technical information like band frequencies, spectral resolution, noise equivalent brightness temperatures (NET), as well as weight and dimensions is given in Table 1. The receiver noise temperatures of the millimetre-wave channels in single sideband mode are of the order of 20 000 K. This high value is to a large extent due to losses in the dielectric sideband filters. A foreseen upgrade of the receivers is expected to bring this value down to ∼5000 K, at which a NET of 1 K can be achieved. In the mean time, an average of 8 scans taken at NETs of 4–6 K each is taken to produce equivalent result.

2.2 Millimetre-wave radiometer

The primary subsystem in MARSCHALS is the millimetre wave radiometer, shown schematically in Fig. 2.

The input to the three millimetre wave receivers can be selected through a switching mirror among the following three targets: atmospheric limb, cold blackbody target, or hot blackbody target. The available spectrometer bandwidth is only sufficient for one band at a time, so a band switch following each receiver couples the IF output from each of the receivers in turn to the IF processing electronics and channeliser spectrometer. Observation time for each of bands B, C and D is normally shared equally.

2.3 Radiometric calibration

High elevation angle views of the sky are sufficiently contaminated by spectral features, even if the instrument flies at 35km altitude, that they are unsuitable for use in calibrating the MARSCHALS instrument. MARSCHALS therefore employs two onboard radiometric calibration targets: one at ambient temperature and one cooled using liquid argon to approximately 86K.

A rotating mirror is used to switch between the two calibration targets and the sky view during the limb scan. The switching sequence is completely programmable to allow for modifications in the light of system performance.

2.4 Antenna pointing system

To improve accuracy of atmospheric constituent profile retrievals, a closed-loop control system is used to stabilize the line of sight of the MARSCHALS mm-wave receivers.

A brushless motor is used to position the antenna, driven by a custom-designed controller, with an Inductosyn™ sensor mounted directly to the driveshaft providing positional feedback. Due to the requirement for highly accurate (0.0025° rms) knowledge of the pointing, a dedicated IMU is mounted on the MARSCHALS instrument frame. Both the IMU and the Inductosyn™ have resolutions $\ll$1 arcsec, and the control loop has been demonstrated in flight to achieve settling time $<$0.25s and jitter $<$0.01°.

The Antenna Pointing System (APS) additionally receives an aircraft roll angle update from the Geophysica UCSE (Unit for Connection of Scientific Equipment) telemetry module. The APS compares this value of aircraft roll angle with the value from its own IMU and uses it to correct for any long term drift in the IMU.

2.5 Optical cloud monitor

Positioned just above the mm-wave scanning antenna, and viewing through the same aircraft aperture, the OCM comprises a CCD (charge-coupled device) imager with good near-infrared responsivity fitted with an 850 nm filter. The camera has a fixed FOV of approximately 6.6° in the vertical plane, centred at a declination of 2.9° below horizontal; the vertical FOV therefore includes in a single frame the complete mm-wave FOV observed during a limb scan. Further details can be found in Moyna et al. (2006).

3 The SCOUT-O3 campaign in Darwin

This paper reports the results obtained by MARSCHALS during the SCOUT-O3 campaign in Darwin. The aim of the SCOUT-O3 project is to provide scientific knowledge for global assessments on ozone depletion and climate change for the Montreal and Kyoto Protocols and to achieve a better understanding of processes, both chemical and dynamical, occurring in the UTLS region. In December 2005 the combined SCOUT-O3/ACTIVE campaign (Vaughan et al., 2007) took place in Darwin (12.47° S, 130.85° E), Australia, with the aim of studying the chemical composition of the TTL and the convective Stratosphere-Troposphere Exchange (STE) caused by the powerful thunderstorm system called Hector that occurs almost daily over the Tiwi islands immediately north of Darwin. The SCOUT-O3 team was present at Darwin with two aircrafts, the M55 Geophysica (flight altitude up to 20 km) and the DLR Falcon (up to 12 km). The ACTIVE team was deploying the Australien Grob G520T Egrett (up to 14 km) and NERC's Dornier-228 (up to 4 km). During the measurement campaign the M55 performed 9 local flights in Australia. The M55 payload varied from flight to flight and was made of several in-situ instruments and of the four limb sounders: MIPAS-STR (Michelson Interferometer for Passive Atmospheric Sounding-STRatospheric aircraft), CRISTA-NF (Cryogenic Infrared Spectrometers and Telescopes for the Atmosphere-New Frontiers), MTP (Microwave Temperature Profiler) and MARSCHALS. In the flights when MARSCHALS was on board of the M55, MTP measured Temperature, CRISTA-NF provided data for the cloud coverage only, while both MARSCHALS and MIPAS-STR measured altitude distribution profiles of Temperature and some molecules among which H_2O, O_3 and HNO_3 are common.

3.1 MARSCHALS measurements

MARSCHALS was deployed on the four local flights numbered 4, 5, 6 and 9. The corresponding flight dates are the 25th, 28th and 29th November 2005 and the 5th December 2005. Flight 4 on the 25th November was the first ever scientific deployment of MARSCHALS and atmospheric spectra have been recorded for the whole duration of the flight. Although this was a great success, flight 4 was a Hector flight the particular flight pattern used for cloud sampling with numerous and frequent changes in direction and flight altitude made it particularly unsuitable for remote sensing applications. On flight 5 on the 18th Nov the aircraft was forced to land immediately after take-off because its transponder failed to work and as a result no scientific measurements could be taken. On flight 6 of 29th November MARSCHALS was recording a full set of OCM cloud measurements, geolocation, housekeeping and aircraft UCSE data but, due to an error in the antenna controller, the scanning mirror could not be stabilised and no atmospheric data were measured. Prior to the last deployment some improvised in-field repairs to the pointing system have been performed. For flight 9 on 5th December the pointing system was working again, but it was now using fixed command angles and did not provide active antenna control to compensate for aircraft roll. The aircraft flight attitude was nevertheless independently recorded both by the MARSCHALS inertial navigation system (consisting of two gyroscopes and 3 accelerometers), as well as by the

aircraft's flight control system (UCSE data). The true view angle was reconstructed to a high level of accuracy from both datasets in the post processing of the data (level1b data) as seen in the results of the pointing retrieval.

During flight 9 MARSCHALS scans were made for about 200 limb views in a single band. The three bands were acquired in subsequent scans: one scan for band B first, then band D and then band C. Band D was not yet operational at the time of this campaign. In band B good spectra were measured at the beginning of the flight, but the receivers proved to be thermally unstable and the quality of the recorded spectra rapidly deteriorated after takeoff in the harsh meteorological condition at high flight altitudes. Thus the results presented in this study are derived from analysing atmospheric spectra measured in band C on the remote sensing flight 9 of 5th December 2005 only.

3.2 MIPAS-STR measurements

MIPAS-STR (Keim et al., 2004) is a cryogenic Fourier Transform emission sounder operating in the middle infrared. The instrument allows limb and upward viewing, yielding about 2 km vertical resolution below the Geophysica flight level (up to 20 km) and mainly column data above. Reduced vertical information above the flight level is obtained by upward measurements with several elevation angles. Two-sided interferograms were obtained with a maximum optical path difference L of 12.5 cm, resulting in a spectral resolution (1/2L) of 0.04 cm^{-1}. For a flight altitude of 19 km the complete sequence, including calibration, takes 200 s. This results in a horizontal resolution in flight direction of about 36 km.

During flight 9 MIPAS-STR performed perfectly and made continuous limb measurements. During the dive the shutters were closed to avoid condensation of water inside the cold optic module. In total some 50 limb scans have been measured. MIPAS-STR measurements were simultaneously made in the same direction of MARSCHALS and an excellent coincidence in time and space of both limb sounders is evident. On average there are about 3 limb scans of MIPAS-STR for each limb scan of MARSCHALS.

The atmospheric conditions made the analysis of MIPAS-STR data extremely difficult. This was mainly because of the presence of optically thick clouds in the infra-red during large parts of the flight. Figure 3 shows the distribution along the flight track of the Cloud-Index (CI) defined as the quotient of the radiance measured by MIPAS-STR at 830 cm^{-1} and at 791 cm^{-1} (Spang et al., 2004). The CI was derived for each tangent point from the individual MIPAS-STR spectra and a value of 4 was chosen to separate cloudy from no cloudy measurements. The CI plots show the extensive cloud coverage encountered during the flight that was also clearly observed by the Falcon lidar. Nevertheless, as it can be seen in Fig. 3 a few regions in the southern part, close to the dive, apparently gave good signal and have been analysed in detail.

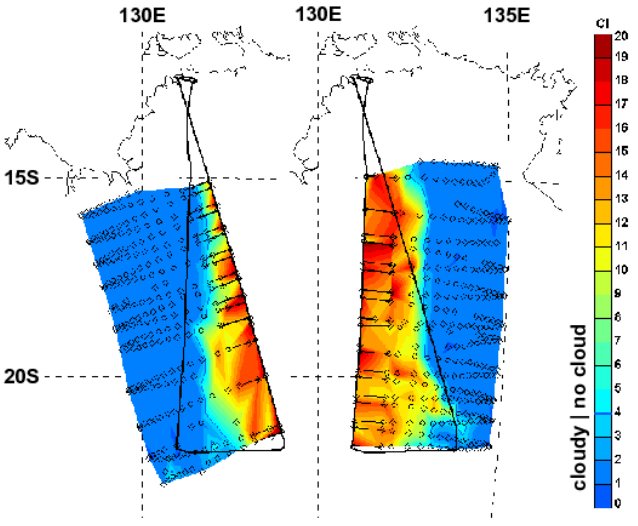

Fig. 3. Flight track of Geophysica on 5 December 2005 and the location of tangent points of the MIPAS-STR instrument. The altitude of the tangent point ranges from 6 km (farthest from the flight track) to flight altitude in 1 km steps. The under-laying field is the distribution of the Cloud Index (CI – quotient of the radiance at 830 cm^{-1} and at 791 cm^{-1}) derived for each tangent point from the individual MIPAS-STR spectrum. A value of 4 was chosen to separate cloud from no cloud.

One of this scans has only a thin aerosol layer at about 14–15 km, which is partly transparent for infrared radiation. Retrievals for aerosol, temperature, CFC-11, CFC-12, HNO_3, O_3, and H_2O have been made for this scan. In the retrieval MIPAS-STR spectra at tangent heights down to 11 km were used.

The error budget of the MIPAS-STR atmospheric profiles is dominated by systematic error sources in the retrieval chain. The error in the used temperature profile is estimated to be within 3 K. The resulting error for the trace gases is estimated by runs with +3 K (−3K respectively) shifted temperature profiles. A second error source is related to the HITRAN spectroscopic line data, and is estimated to be 10% of the VMR. The stability of the pointing is within one arc minute, but the mean deviation is typically derived post-flight from a large set of spectra unaffected by aerosol absorption. The pointing error is therefore estimated conservatively to be 2 mrad (∼7 arc min.), the impact on the VMR profile is determined with retrievals with +2 mrad (−2 mrad respectively) shifted pointing. Compared with the systematic errors, the noise error in the spectra is negligible. To calculate the given maximal(=)total error, all errors have been combined additively. The total (3σ) error of HNO_3 goes from about 50pptv (∼20%) at 10 km to about 700 pptv (∼25%) at 21 km. For ozone, the mixing ratio almost vanishes below 12 km. Until 20 km, the mixing ratios are smaller or comparable to the total errors. The total error of ozone increases from 0.4 ppmv at 10 km, 1.2 ppmv (∼76%) at 21 km to 1.5 ppmv (∼25%) at

25 km. Above the hygropause (14–15 km), the mixing ratio of water is very small, about 2 to 3 times smaller than the errors. Below, the strong gradient makes the water profile sensitive to pointing errors. With decreasing altitude, the mixing ratio increases faster than the errors, at 12 km the errors and the values become equal.

At the lowest point of the profile (10 km), the total error for water mixing ratio is 200 ppm (∼35%).

4 The retrieval code

A dedicated code, named MARC, was developed for the retrieval of the vertical profiles of the target quantities from the calibrated and geolocated spectra measured by MARSCHALS. MARC is a global-fit (see Carlotti et al., 1988), multi-target (see Dinelli et al., 2003) retrieval, in which forward model errors can be accounted for in the inversion process and the Optimal Estimation Method (OEM, see Rodgers, 1997) is used. It can be used for a wide-band analysis of the observations and accounts for horizontal gradients and cloud contamination. This implies that all the measured spectral channels and all the limb angles are simultaneously analysed for the retrieval of all the targets of the observation. The retrieval procedure has been designed to allow the use in the inversion procedure of the full Variance-Covariance Matrix (VCM) (Rodgers, 1997) that includes the spectral errors as well as the forward model errors. As a result, the final retrieval error is the total error budget that is the combination of the random component due to the measurement noise with the systematic components. MARC uses the initial guess of the atmospheric status not only as a starting point of the iterative retrieval, but also as a-priori knowledge of the unknowns (optimal estimation).The shape of the a-priori profile (that extends far above and below the vertical retrieval range) is retained above and below the vertical retrieval range. Further details of the retrieval code can be found in Carli et al. (2007). The forward model inside MARC has the capability of modelling the molecular continuum, and at the same time also a frequency independent absorption profile (external continuum) can be fitted to the data. On the other hand, the effects of the presence of clouds in the field of view of the instrument can be modelled inside the forward model of MARC, but the cloud modelling parameters cannot be a target of the retrieval procedure. This implies that if a cloud is present in the line of sight of the measurements, its effect is in first approximation modelled with the retrieval of an external continuum profile (see Del Bianco et al., 2007) and only in a subsequent retrieval a rigorous modelling of the cloud is attempted. Besides the vertical profiles of the selected atmospheric quantities (temperature, VMRs, external continuum absorption coefficient) MARC can retrieve instrumental scalar quantities in the form of single values for all the spectra of the same scan: one pointing bias value to account for the errors in determining the real pointing of the antenna, a radiometric offset value to be added to all the spectra of the same scan and a correction factor to be multiplied to all the spectra of the same scan to account for detector non-linearity.

For the retrieval diagnostic MARC computes the following quantifiers:

1. The reduced chi-square (χ^2-test) defined as χ^2 − test=$(\boldsymbol{n}^{\mathbf{T}}\mathbf{S}_{\boldsymbol{n}}^{-\mathbf{1}}\boldsymbol{n})/(m-n)$, where m is the number of observations, n is the number of retrieved parameters, $\boldsymbol{n}$ is a vector containing the differences between each observation and the corresponding simulation, and $\mathbf{S}_{\boldsymbol{n}}$ is the VCM of the observations). The χ^2-test has an expectation value of 1. Therefore its value is a good estimate of the quality of the retrieval.

2. The "individual information content" q_j defined as:

$$q_j = -\ln_2\left(\frac{S_{r_j}}{S_{a_j}}\right)$$

Where S_{r_j} is the diagonal element of the VCM of the retrieval and S_{a_j} is the diagonal element of the a-priori covariance matrix. This quantifier gives a measure, in terms of binary bits of information, of the 'gain' provided by the measurement with respect to the a-priori knowledge of each retrieved value (Rodgers, 1998). The value of q_j depends on the a-priori errors chosen for the retrieval, so it is not an absolute quantifier. If the retrieval error is equal to the a-priori error, that is if there is no information in the measurement for the j parameter, q_j is equal to zero. Any other value indicates that some information about the retrieved quantity was present in the measurement. However we consider q_j values below 1 a indication that the retrieved value comes mainly from the a-priori knowledge of the target.

1. The trace, defined as the sum of the diagonal elements, of the Averaging Kernel Matrix ($\mathbf{A_{AKM}}$) (see Rodgers, 2000). This quantity measures the number of independent pieces of information present in the analysed set of measurements (degrees of freedom).

2. The information content of the measurements, defined as $H = -\frac{1}{2}\ln_2|\mathbf{I} - \mathbf{A_{AKM}}|$ where $||$ indicates the determinant of the matrix, see Rodgers, 2000.

5 MARSCHALS data analysis

5.1 Level 1 data

Besides measuring the atmospheric radiance in the millimetre wave region, MARSCHALS also records information on the geolocation and the flight attitude of the observation platform. In addition to this, a near infrared image of the field of view is taken by OCM and saved at a current rate of 1 frame

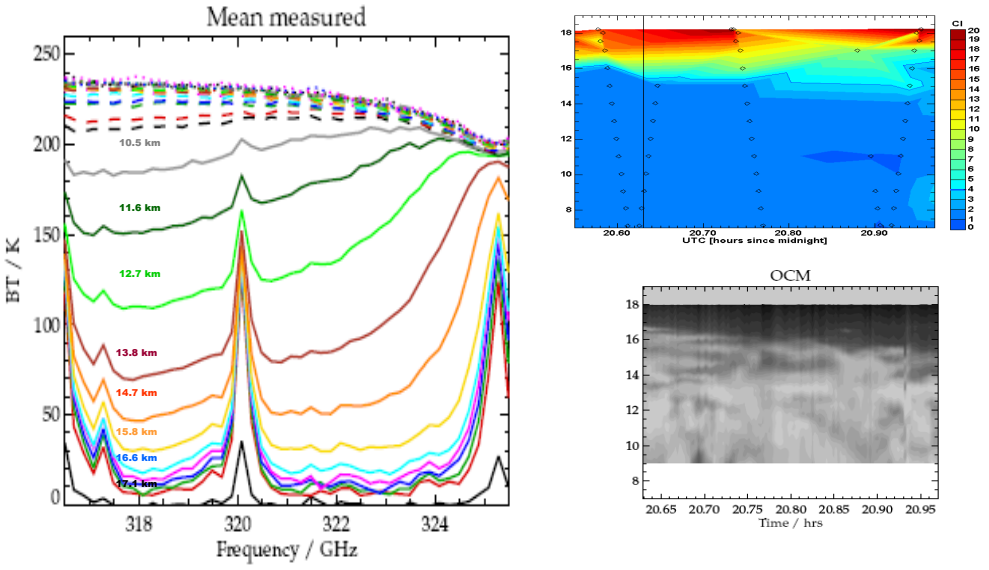

Fig. 4. Left panel: Measured MARSCHALS Brightness Temperature spectra for Band C featuring H_2O at 325 GHZ and O_3 at 320 GHz. All spectra are acquired during an 18 min period of level flight attitude and mean values around nominal view angles are calculated. The multi-coloured numbers in the left panel denote the respective tangent point altitudes of the measurements. The upper right panel shows MIPAS-STR CI (values below 4 indicate the presence of clouds) and the lower right panel show OCM (near-infrared) cloudiness during the same 18 min flight period. Note that spectral line features first become visible at around 10.5 km tangent point altitude. At this altitude and up to the Tropopause at around 16 km there are nevertheless significant amounts of clouds present in the field of view!

per each atmospheric integration cycle (in contrast to the calibration views during which no OCM image are taken). The aim of this is to have an independent assessment of the cloudiness when analysing the millimetre wave data. The MARSCHALS level1 processor calibrates the raw data by means of the internal calibration targets to obtain the spectral radiance in units of brightness temperature. Based on the commanded view angle and the measured platform attitude both tangent point altitude and location are calculated. On flight 9 of 5th December pointing knowledge was reconstituted post flight from gyro and UCSE measurements of the aircraft roll. A common value of the pointing bias for each scan is retrieved in this analysis and the results (see Sect. 5.5) show that the pointing knowledge derived this way is very accurate.

The standard deviation of one calibrated spectrum of 250ms integration time is of the order of 4 K, which is in accordance with the expected noise equivalent brightness temperature (NEBT) of the receiver. The frames taken by the OCM can be collated (after applying the same view angle correction used to derive absolute pointing knowledge) to give a full 2-D picture of the cloudiness in the field of view. The OCM measurements indicate that during the flight clouds were omnipresent at all altitudes below the tropopause height of 17 km. The lowest cloud level is observed in the midsection of the flight. This is indeed the only section of the flight where the infrared receiver MIPAS-STR was able to perform successful atmospheric measurements. The left panel of Fig. 4 shows an example of the measured submillimetre spectra. The spectra shown in the figure were observed during an 18 min period of level flight attitude and mean values around nominal view angles were calculated. The multi-coloured numbers in the left panel denote the respective tangent point altitudes of the measurements. The lower right panel of Fig. 4 shows the OCM cloudiness during the same 18 min flight period. In this picture black colour denotes the cold sky and white/grey colours denote clouds of varying optical thickness. The upper right panel of Fig. 4 reports the CI measured by MIPAS-STR for the same flight period. The comparison of MARSCHALS spectra and both the OCM cloud picture and MIPAS-STR CI in Fig. 4 shows that spectral features visible in the range between 10.5 km and 17 km have been recorded in the occurrence of substantial cloud coverage.

5.2 Analysed dataset

As we have seen in Sect. 3.3, band B performances were poor and only Band C data for the flight of the 5 December 2005 have been analysed. The upper panel of Fig. 5 shows the position of the aircraft during flight 9 and, in different colours, the geolocation of the tangent points of the Band C scans, while the lower panel of the same figure shows the flight altitude plotted versus the universal time coordinate with the Band C scan numbers reported on top. The analysis has been performed on scans from 3 to 24 and from 36 to 54. Scans

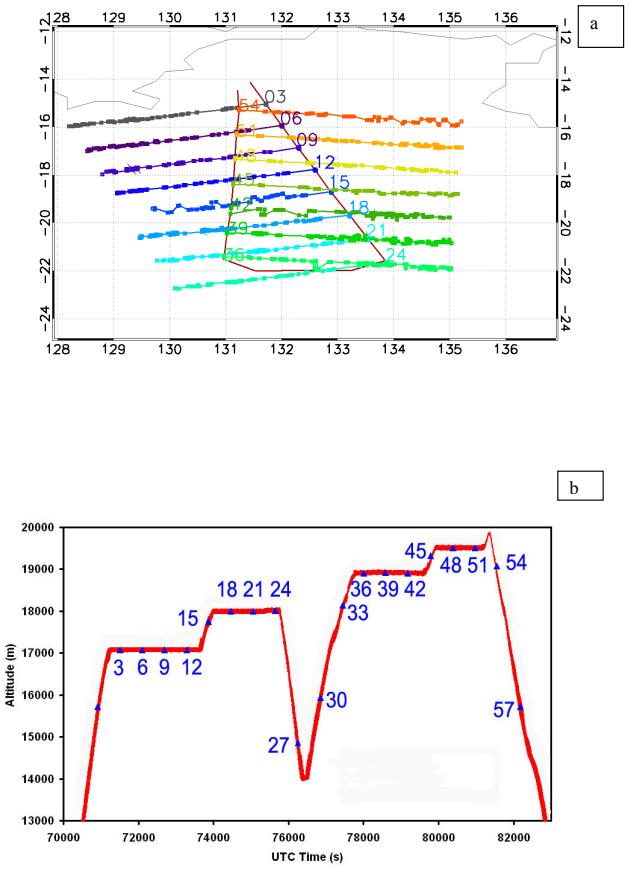

Fig. 5. **(a)** The flight track plotted versus latitude and longitude. Only the positions of the tangent points of band C scans are reported in different colors. **(b)** The flight altitude (m) and band C scan position plotted versus the Universal Time Coordinate (UTC).

0, 27, 30, 33, and 57, which have been acquired during the ascent, dive, and descent of the aircraft, have been discarded on account of artefacts of the varying platform altitude.

Since some of the acquired spectra were very noisy and because we had a redundancy of sweeps (see Sect. 3.2), spectra with the average noise level above 8 K have been discarded.

5.3 Initial status of the atmosphere

As stated in Sect. 4, the code MARC uses the initial status of the atmosphere as a-priori knowledge of the retrieval targets. This implies that the initial atmospheric status should be as close as possible to the true status of the atmosphere in order to have a good a-priori estimate of the profiles that are the retrieval targets and to minimize the impact of interfering species that are not a retrieval target. A good estimate of pressure and temperature for the time and location of the measurements can be provided by ECMWF. ECMWF provides also data for water and ozone. For all the other gases emitting in the spectral region measured by MARSCHALS, the IG2 database (a database containing average atmospheric profiles along with their 1-sigma variability that was developed by J. Remedios (Remedios, 1999) for the analysis of MIPAS/ENVISAT spectra) for an equatorial atmosphere was used. ECMWF data were extracted from the MARS Archive (Meteorological Archival and Retrieval System). The MARS Archive provides data for Geopotential (m^2/s^2), Temperature (K), Specific Humidity (Q) (kg/kg) and Ozone Mass Mixing Ratio (MMR) (kg/kg) on a chosen latitude-longitude grid and on user defined pressure levels while the IG2 database contains average profiles for all species over a wide latitude band. We have extracted from the archive the data for December 5, 2005 (the date of the flight) at 18:00 and 24:00 UTC at steps of 1° in both latitude-longitude from latitude −13° to −23° and from longitude 128° to 134°. The extracted ECMWF profiles were interpolated in latitude, longitude and time in order to obtain the profiles at the time and at the average geo-locations of MARSCHALS scans. The data for Q and Ozone MMR have been converted into H_2O and O_3 VMR profiles.

Since the OEM uses the errors associated with the a-priori profiles as the weight with which the a-priori information is combined with the measurement information, particular care should be used in their choice. For all the target species but temperature, in our analysis we have used the measured atmospheric 1-σ variability that has been estimated by Remedios (1999) for the latitude band of Darwin and that is included in the IG2 database. Only for the temperature, whose knowledge is supposed to be better than the registered variability over the wide latitude band considered in the IG2 database, a 3 K constant error was used. In the altitude range of MARSCHALS measurements the size of the a-priori errors for water ranged from 10% at 23 km to 190% at 7 km; for ozone the a-priori errors ranged from 30% to 100% depending on the altitude and for HNO3 the errors ranged from 40% to 100%.

5.4 Retrieval setup

The targets of MARSCHALS measurements, when operating on all the three bands, have been identified during the theoretical retrieval study performed on a mid-latitude and polar atmosphere for the development of the MARC code (Dinelli et al., 2007)to be the altitude distributions of T, H_2O, O_3, HNO_3, N_2O, CO and of the external continuum (Multi Target Retrieval) and the scalar values (that is a single value that is applied to each sweep of the scan) of the pointing bias, instrumental offset and gain correction factor (see Sect. 4 for their definition). For the retrieval of band C measurements only, during the same study the identified targets were: the altitude distributions of T, H_2O, O_3, HNO_3 and of the external continuum plus all the three scalar values.

Common retrieval options adopted for all the analysed scans were:

– Same vertical retrieval grid (target dependent)

– Upper limit of the radiative transfer integral 50 km

– Use of the Optimal Estimation Method (OEM)

– No hydrostatic equilibrium (the initial pressure and temperature profiles have been assumed to be in hydrostatic equilibrium. However the hydrostatic equilibrium has not been forced during the iterative procedure because anomalous T values could cause the reconstruction of wrong pressures therefore affecting the quality of the retrieval).

Tests have been performed to check if the above mentioned targets could all be retrieved, and to tune the vertical retrieval grid of each target and the best altitude range of the analysed measurements. After all the performed tests we have defined a final retrieval setup that ensures the best results for the analysis of band C spectra:

– Spectra have been selected according to the following criteria: Tangent altitude >6 km, Average Noise <8 K

– Use of GPS altitudes as flight altitudes of the aircraft

– Use average noise values without correlations among the sweeps that share the same calibration view

– Spectra that after a first run of the retrieval had χ^2-test values higher than 20 have been removed from the analysis

The best vertical retrieval grid (which has been kept constant throughout the whole flight) was determined for each target as a compromise between the number of altitudes needed for a correct representation of the vertical profile and the "individual information content" (see Sect. 4) of the measurements. For all the targets we have performed the retrieval in the altitude range sampled by the instrument plus a couple of altitudes above the highest flight altitude (where the information content of the measurements is always very low). This was done to avoid errors introduced in the retrieved profiles by the assumed vertical distribution above the topmost retrieved point. The same applies to the lower part of all the retrieved profiles.

Since sub-millimetre measurements are not very sensitive to the temperature, and therefore the error with which it can be retrieved is high, we have privileged to maintain a detailed representation of the profile rather than to pursuit the innovative information content of the measurements and we have chosen a vertical grid made of 10 points at 7, 9, 11, 13, 15, 17, 19, 20, 22, 26 km. For water vapour we have chosen a vertical retrieval grid made of 15 points with steps of 1 km from 8 to 20 km plus two points at 23 and 26 km in order to have reasonable individual information content and a good representation of the profile around the hydropause. Ozone

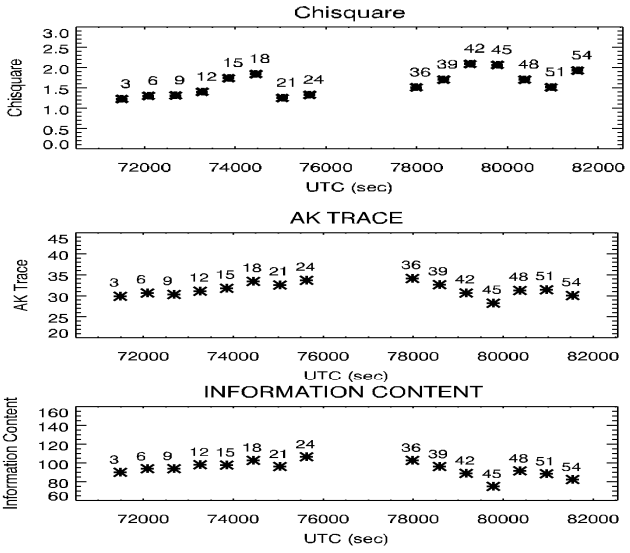

Fig. 6.
Final χ^2-Test value, $\mathbf{A_{AKM}}$ trace and information content for the analysis of band C for each scan reported as a function of the acquisition time (UTC).

was retrieved on 12 points at 7, 10, 13, 14, 15, 16, 17, 18, 19, 20, 23 and 26 km while HNO_3 vertical grid was made of 8 points at 9, 11, 14, 16, 18, 19, 20 and 24 km. The external continuum was retrieved at 1 km step from 7 to 19 km.

5.5 Retrieval results

The upper panel of Fig. 6 reports the final χ^2-test values obtained in the analysis of each scan. The χ^2-test value is always close to 1, indicating the presence of low systematic errors and validating the choice of the use of a single noise value for each sweep in the retrieval. The central and lower panels of Fig. 6 show the retrieval quantifiers relative to the analysis of each scan. Both the trace of the $\mathbf{A_{AKM}}$ matrix and the information content of the measurements are fairly constant throughout the whole flight, indicating the constant quality of the measurements. In Table 2 we report the retrieval performances in terms of degrees of freedom and obtained accuracy of the band C analysis for each target; the degrees of freedom of the different targets obtained in the analysis of each scan are plotted in Fig. 7. The figure highlights that, despite the variable flight altitude and the cloud coverage, good and stable results have been obtained.

The results of the analysis are mapped in Figs. 8 to 12. Each figure shows the 3-D maps of the targets (VMR, T, external continuum), of their retrieval error and of the individual information content (q_j) plotted versus altitude and acquisition time. On each map the black line shows the altitude of the instrument and the white dots show the altitudes at which the retrieval was performed. Pointing bias, offset and gain (shown in Figures 13 top, central, and bottom panels

Table 2. Average performances of the retrieval of band C.

Species	Number of retrieved altitudes (parameters)	Degrees of Freedom	Altitude [Km]	Accuracy [%]
Temperature	10	4	Flight altitude to 10 km	–
H_2O	15	10–11	flight altitude to 12 km	10
O_3	12	6.5	flight altitude to 4 km below	10–60
HNO_3	8	2	flight altitude to 2 km below	40–60
Continuum	13	5	Flight altitude to 15 km	–
Scalar quantities	3	3		
Total	58	31		

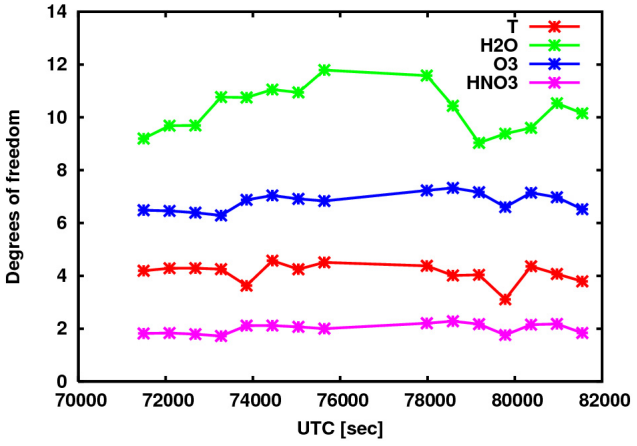

Fig. 7. Degrees of freedom for the different targets plotted as a function of the acquisition time (UTC).

respectively) are always very well determined. The average retrieved pointing bias is 3±10 mdeg, which compares well with the 2.5 mdeg rms pointing knowledge during a scan reported in the instrument specifications (see. Sect. 2.2.). The average retrieved gain correction is 0.999±0007, indicating that the detector response had no deviations from linearity. The average retrieved offset is 0.15±0.45 K, indicating that the instrument was not affected by the different environmental conditions encountered during the flight (i.e. the strong temperature variations experienced during the dive).

As it can be seen in the map of the "individual information content" shown in Fig. 8, the temperature is mainly determined by the a-priori information (q_j values below 1 bit of information above 15 km and below 10 km), as it is suggested by the comparison in Table 2 of the number of degrees of freedom of the temperature retrieval (also shown by the red line of Fig. 7) with the number of altitudes at which the temperature is retrieved. This is the result of the choice of a retrieval grid which, for a quantity that is not the main target of sub-millimetre measurements, gives priority to the details of the profile. However some contributions of the measurements are present from 16 km down to about 10 Km depending on the scan.

As it can be seen in Table 2 and as shown by the green line of Fig. 7, the degrees of freedom for water are slightly lower than the number of altitudes at which the retrieval is performed. This is due to the choice of a vertical retrieval grid that is driven by the necessity to have a detailed water profile around the hydropause. However this does not compromise the quality of the retrieval, as shown by the maps of Fig. 9. The map of the individual information content shows that the H_2O profiles are well determined from flight altitude down to about 10 km where we gain up to 2 bit of information with respect to the expected value coming from climatology. The accuracy obtained over that altitude range is about 10% (see Table 2).

The ozone profiles (see Fig. 10) are well determined in an altitude strip that goes from flight altitude down to 14 km with an accuracy that varies from 10% near the aircraft to 60% at the lowest altitude (see Table 2). This is a remarkable result if we think that the ozone concentration below the tropopause is always very low and that for most of the flight the aircraft was flying in the tropopause region. We can see that at the very end of the flight, when the aircraft finally flies above the tropopause, the altitude strip where the individual information content of the ozone profiles is above 1 gets wider.

The HNO_3 profiles (Fig. 11) are always poorly determined (its accuracy is never better than 40% – see Table 2) due to the low signal to noise ratio of its emission in the analysed spectral region, probably because of the high altitude of the tropopause with respect to the position of the instrument at these latitudes and time of the year. In fact we can clearly see an enhancement of the individual information content of the measurements after scan 12 (073270 UTC when the flight altitude goes from 17 to 18 km). In the second part of the flight, when the aircraft flies well above the tropopause, there is a little more information for this target also above the aircraft.

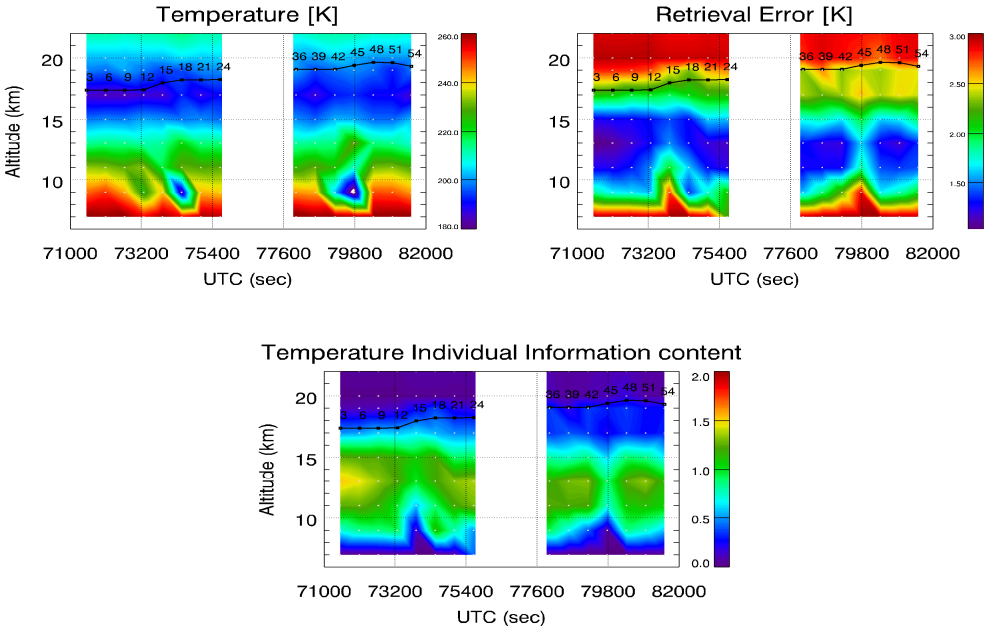

Fig. 8. Retrieved Temperature [K] using the scans of band C (top-left panel), the related retrieval error [K] (top-right) and the individual information content of the measurements (bottom). The grey dots show the retrieval grid and the black line shows the aircraft altitude.

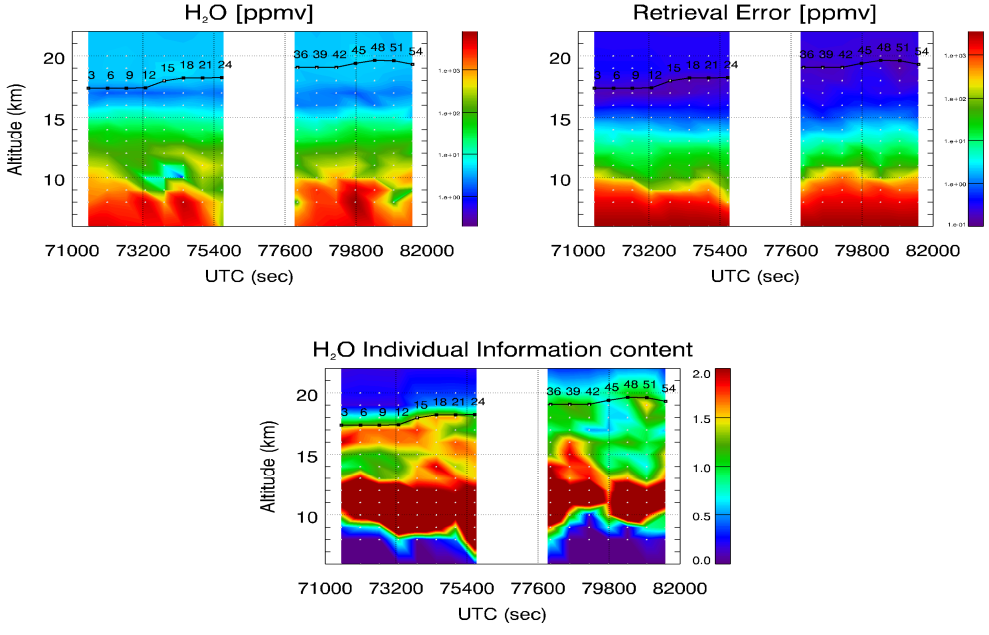

Fig. 9. Retrieved H_2O [ppmV] using the scans of band C (top-left panel), the related retrieval error [ppmV] (top-right panel) and the individual information content (bottom panel). The grey dots show the retrieval grid and the black line shows the aircraft altitude.

As an example of the results of the analysis, the individual profiles and the Averaging Kernels (AK) for scan 51 are plotted in Fig. 14. In the 4 panels of the figure reporting the VMR profiles, the solid line represents the retrieved profile, the dashed line is the initial guess (a-priori) profile and the dotted lines, showing the a-priori profile plus/minus the a-priori errors, are drawn to show the size of the a-priori errors used to weight the a-priori information in the retrieval. The black dashed line indicates the average altitude of the instrument during the scan. In the 4 panels showing the AK of the retrieved values, each AK is plotted in a different colour: in the legend we have used the same colour to report the altitude of the parameter which the AK is referred to.

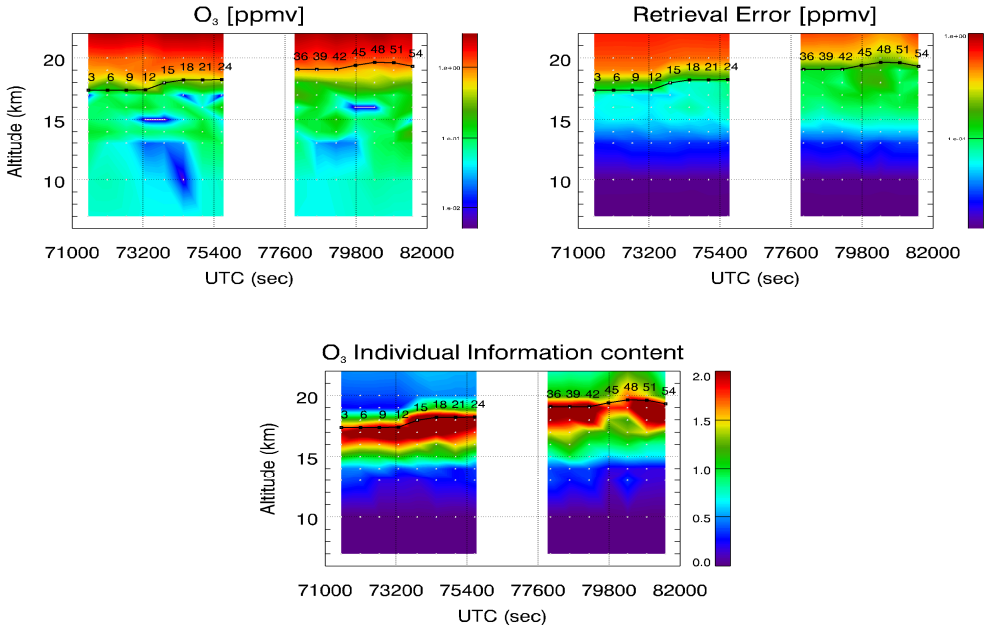

Fig. 10. Retrieved O_3 [ppmV] using the scans of band C (top-left panel), the related retrieval error [ppmV] (top-right panel) and the individual information content (bottom). The grey dots show the retrieval grid and the black line shows the aircraft altitude.

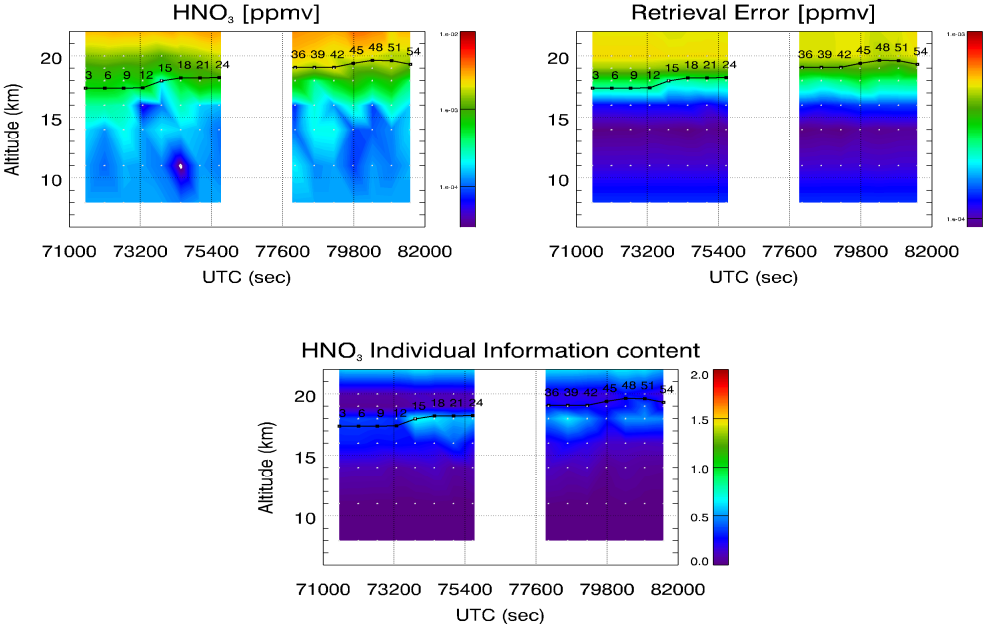

Fig. 11. Retrieved HNO_3 [ppmV] using the scans of band C (top-left panel), the related retrieval error [ppmV] (top-right panel) and the individual information content (bottom panel). The grey dots show the retrieval grid and the black line shows the aircraft altitude.

Even if the information content of the measurements for the temperature at 9 km is low, the low temperature values found at that altitude for scans 18 (074445 UTC), 42 (79180 UTC) and 45 (79780 UTC) (see Fig. 8), that sample the atmosphere at the same latitudes, suggest the presence of an intrusion of stratospheric air into the troposphere. This is confirmed also by the low values found at the same altitudes for the water vapour (see Fig. 9).

The results obtained in this analysis are in agreement with the findings of the theoretical retrieval study (Dinelli et al., 2007) performed to assess the measurements capability of MARSCHALS+MARC, despite the fact that the measure-

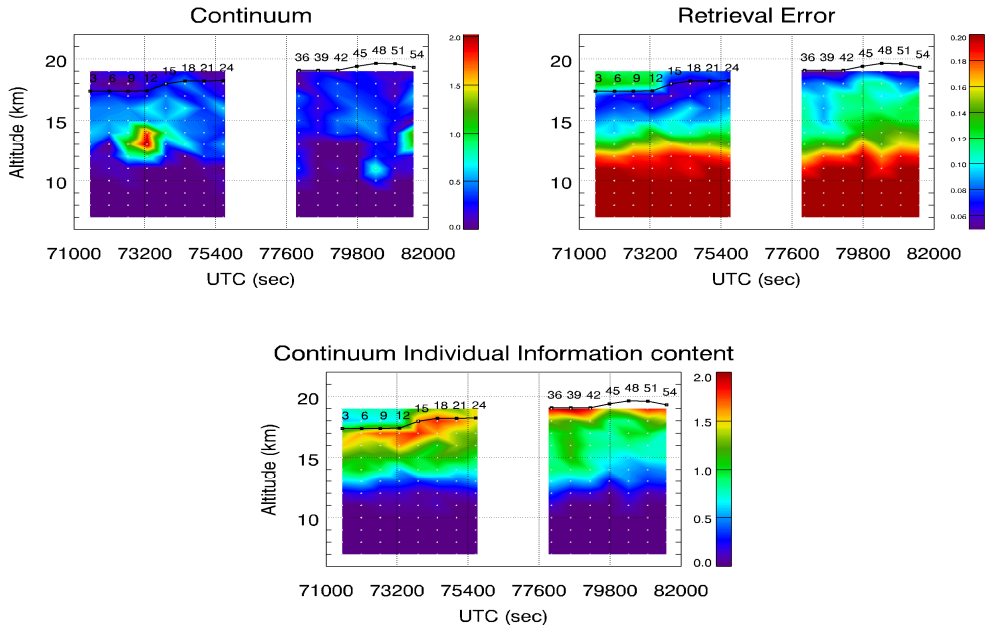

Fig. 12. Retrieved un-accounted continuum [1027 cm^2] using the scans of band C (top-left panel), the related retrieval error [1027 cm^2] (top-right panel) and the individual information content (bottom panel). The grey dots show the retrieval grid and the black line shows the aircraft altitude.

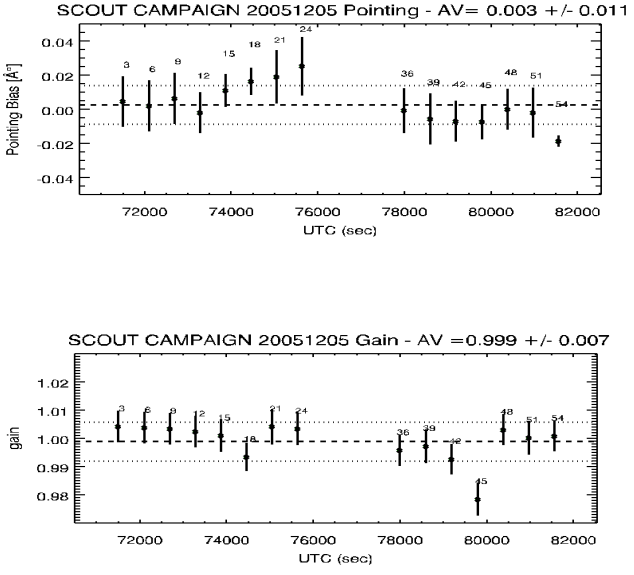

Fig. 13. Retrieved pointing bias (top panel), gain (central panel) and offset (bottom panel) using the scans of band C. The quantities are plotted versus the acquisition time (UTC). The dashed line represents their average value and the dotted lines represent the relative ESD.

ment strategy was completely different from the assumed one and that the study was performed for a mid-latitude atmosphere with the aircraft altitude much higher than the real one. MARSCHALS was required to measure water vapour, ozone, nitric acid N_2O and carbon monoxide in the UTLS region. With the lack of two bands and with a much lower S/N it has been possible to retrieve with sufficient accuracy the targets whose spectral features were present in the measured band above the noise.

The retrieval of the external continuum (see Figure 12) highlights that, with the exception of some absorption observed around scan 12 (73270 UTC), the clouds, whose presence was reported by other instruments such as the OCM imager, MIPAS-STR and the lidar on board the Falcon aircraft, were not affecting the millimetre waves measurement. The loss of sensitivity at about 10 km occurs because of the high absorption of water vapour in the tropical region and not because of the detected cloud coverage.

As shown by Del Bianco et al. (2007), in the millimetre-wave region the clouds can be classified according to their effect in the radiative transfer, into:

1. clouds practically transparent,
2. clouds adequately modelled in the retrieval by the fit of atmospheric continuum absorption,
3. clouds that require the modelling of the scattering effects.

The largest absorption observed in Fig. 12 around scan 12 corresponds to clouds that in the retrieval study of Del Bianco et al. (2007) were located close to the boundary between case b) and c).

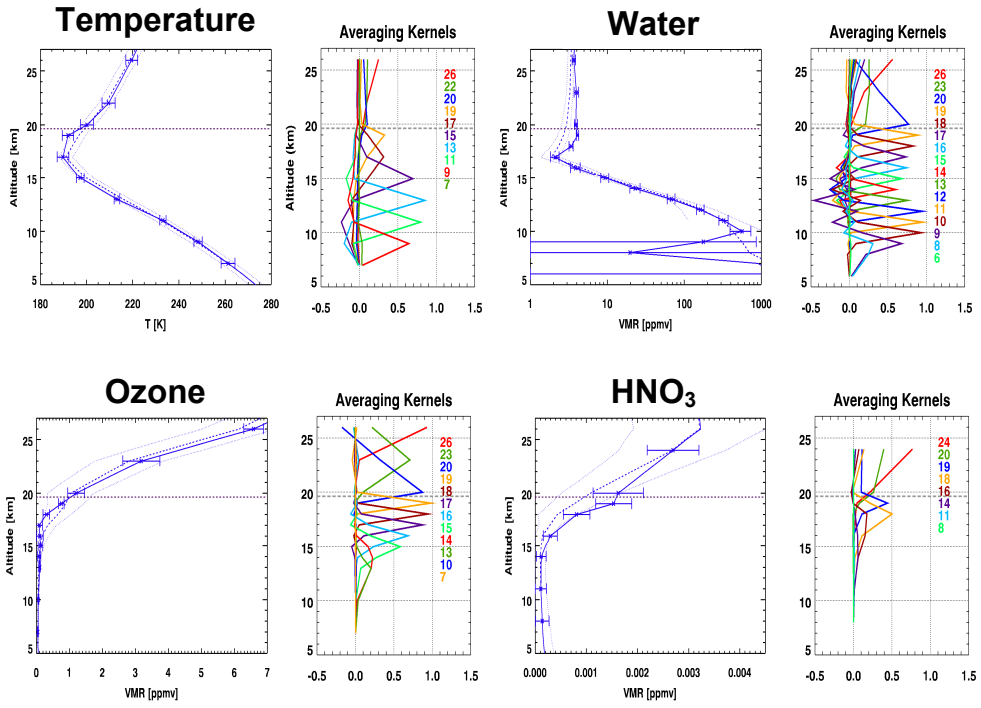

Fig. 14. Results of the analysis of scan 51. For each target the retrieved VMR (left panel) and the relative AK (right panel) are plotted with respect to the altitude. In the right panels, the solid blue line represents the retrieved profile, the dashed line is the initial guess (a-priori) profile and the dotted lines show the boundaries of the a-priori errors applied to the initial guess profile.The black dashed line indicates the average altitude of the instrument during the scan. In the left panel each color corresponds to the AK of the parameter at the altitude listed in the same color in the legend.

Tests have been made repeating the retrieval of scan 12 with a proper scattering model of the cloud. The cloud properties were varied in a range of possible values, but the reduction of the chi-test that was observed for some cloud properties was very small and no significant change was obtained in the retrieved quantities, confirming that also in the case of maximum absorption the cloud was adequately modelled with an atmospheric continuum profile.

6 Intercomparison with MIPAS-STR

The results of our analysis have been validated with measurements of in-situ instruments on board the M55 during the flight. The outcome of this exercise is reported in Dinelli et al., 2007. Here we limit the validation exercise to the comparison of the results obtained from MARSCHALS scans with the profiles obtained by MIPAS-STR (the only limb viewer instrument on board the M55) during the same flight. As already said in Sect. 3.2, one scan only was available for MIPAS-STR. The profiles obtained in the analysis of this scan have been compared with the profiles retrieved from MARSCHALS scans 36 and 39 that have been acquired right before and right after MIPAS-STR scan and therefore sample similar air masses. The results of the comparison are shown in Fig. 15.

The upper left panel of Fig. 15 shows the comparison of the temperature obtained analysing MARSCHALS scans with the temperature profile obtained by MIPAS-STR. In general the profiles agree quite well in the altitude range from 10 to 22 km: the tropopause is found to be located at the same altitude and the profiles lay within their error bars. Above 22 km, where the individual information content is small (see lower panel of Figure 98) and the retrieved profiles are biased toward the a-priori (i.e. the ECMWF profiles obtained as described in Sect. 5), the profiles start to diverge.

The upper right panel of Fig. 15 shows the comparison of scans 36 and 39 with the water vapour VMR profile obtained by MIPAS-STR. From Fig. 9, which shows the individual information content for the water vapour retrievals of MARSCHALS, we can see that the maximum of the information content on water vapour is above 10 km, and unfortunately the error bars of MIPAS-STR data in that region are too large to prevent any conclusion from the comparison. However in the small altitude region where MIPAS-STR profile has low error bars and MARSCHALS data have enough information content, the profiles agree quite well.

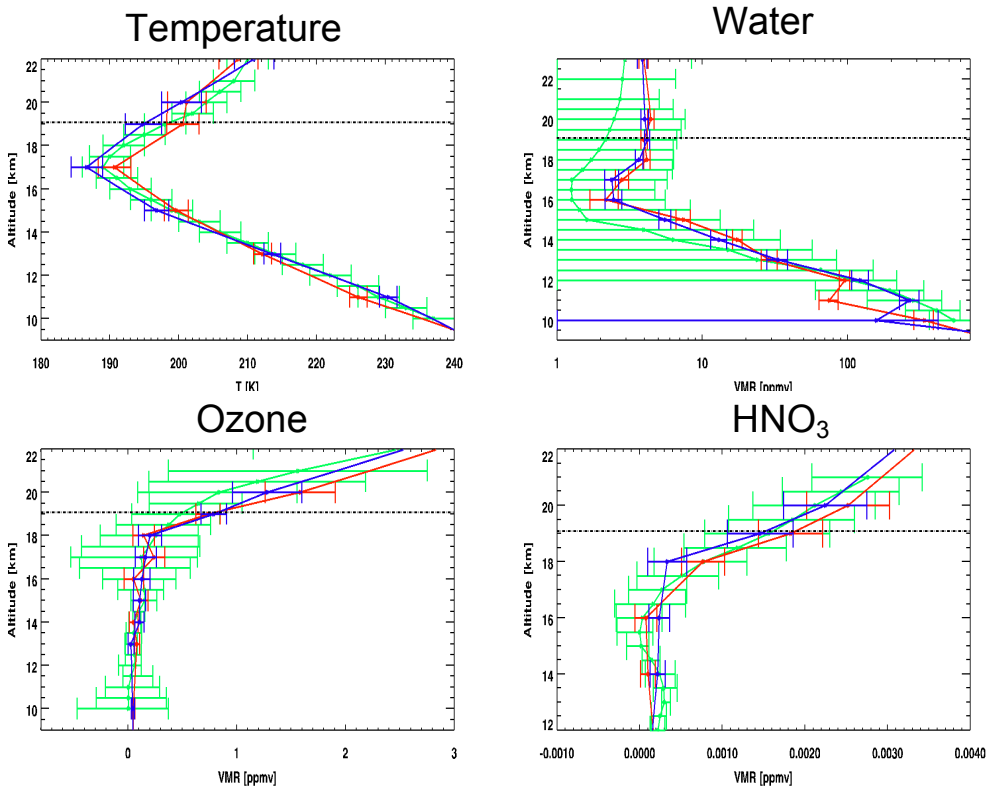

Fig. 15. Comparison of the results of MARSCHALS scans 36 (in red) and 39 (in blue) with MIPAS-STR (in green), together with the total error bars (=3σ).

The lower left panel of Fig. 15 shows the comparison of scans 36 and 39 with the ozone VMR profile obtained by MIPAS-STR. We can see that the agreement is good; the profiles never differ for more than their retrieval error (shown in the figure). MIPAS-STR and MARSCHALS O_3 profiles show discrepancies where the individual information content of MARSCHALS spectra is low, that is when the weight of the a-priori information used in the retrieval starts to increase.

The lower right panel of Fig. 15 shows the comparison of scans 36 and 39 with the HNO_3 VMR profile obtained by MIPAS-STR. The lower panel of Fig. 11 shows the individual information content of MARSCHALS scans for HNO_3. It is clear that the information content of band C for this molecule is lower than for the other examined targets. This means that the a-priori information used in MARSCHALS retrievals always has some influence in the retrieval products. Despite this fact, we can see that MIPAS-STR and MARSCHALS results are in agreement from 15 km upward, and the fact that MARSCHALS fails to catch the structure measured by MIPAS-STR at 14 km is in line with the very low information content at that altitude.

7 Conclusions

First scientific measurements were obtained by MARSCHALS on a stratospheric remote sensing flight from Darwin on 5th December 2005. Atmospheric spectra were recorded in band C at frequencies of 316.5–325.5 GHz. The measurements were affected by a noise level larger than planned (a NET of 4–5 K instead of the value of 1 K used in the case studies of the theoretical retrieval study reported in Dinelli et al., 2007). This shortcoming was partially compensated by the measurement of extra limb views in each limb scan corresponding to a longer measurement time. It was possible to verify with direct evidence the capability of millimetre wave measurements of making minor constituent measurements in presence of clouds that obscure middle infrared instruments. The flight took place above high clouds, which compromised most of the limb measurement of MIPAS-STR, while MARSCHALS was practically unaffected by the clouds. Indeed, most of the time the clouds were practically transparent and only in one scan an absorbing cloud was observed, that was adequately modelled in the retrieval by an external continuum absorption profile. The high concentration of water vapour in the tropical region where the flight took place, rather than the clouds, limited the altitude range

of the retrieval from about 10 km to about flight altitude. Furthermore, while the aircraft altitude ranged from 17 to 19 km, the tropopause was located at about 17 km. Species like ozone and HNO_3 with very low concentrations in the troposphere were only present in abundances above the detection limits of the instrument within a small altitude range. Within the limits of the reduced sensitivity due to the single band measurements and due to the larger spectral error the retrieval performances were consistent with the results expected from the theoretical retrieval study (Dinelli et al., 2007), and H_2O, O_3, and HNO_3 have been measured in the UTLS (Upper Troposphere – Lower Stratosphere).

MARSCHALS profiles have been validated using the measurements acquired by the mid-IR instrument MIPAS-STR. The ubiquitous cloud coverage observed during the flight affected the measurement capability of MIPAS-STR. As a consequence, data taken from the analysis of one single scan were available for the intercomparison. For the scans sampling the same air masses the results obtained by the two instruments are in good agreement. The performed analysis of MARSCHALS data shows that the instrument is capable of measuring the atmospheric composition in the UTLS region, even in presence of clouds that are optically thick at IR wavelengths.

Acknowledgements. This work was funded by ESA ESTEC/Contract 16530/02/NL/MM

MARSCHALS was funded by the European Space Agency ESA, as was its deployment in SCOUT-O3 Darwin.

We thank ECMWF for having granted direct access to their archives of atmospheric data.

We thank Gregory Cailley for his work on the MARSCHALS level1 processor and J. Langen for his useful comments.

Edited by: S. Buehler

References

Barath, F. T., Chavez, M. C., Cofield, R. E., et al., The Upper Atmosphere Research Satellite Microwave Limb Sounder Instrument, J. Geophys. Res., 98(D6), 10751–10762, 1993.

Blumstein, D., Chalon, G., Carlier, T., Buil, C., Hébert, P., Maciaszek, T., Ponce, G., Phulpin, T., Tournier, B., Siméoni, D., et al.: IASI instrument: Technical Overview and measured performances, SPIE Conference, Denver, CO, USA, SPIE 2004-5543-222004, August 2004.

Boone, C., Nassar, R., McLeod, S., Walker, K., and Bernath, P.: Scisat-1 retrieval results, Proc. SPIE, 5542; 184–194, 2004.

Carli, B., Bazzini, G., Castelli, E., Cecchi-Pestellini, C., Del Bianco, S., Dinelli, B. M., Gai, M., Magnani, L., Ridolfi, M., and Santurri, L.: MARC: a code for the retrieval of atmospheric parameters from millimetrewave limb measurements, J. Quant. Spectrosc. Radiat. Transfer., 105, 476–491, 2007.

Carlotti, M.: Global-fit approach to the analysis of limb-scanning atmospheric measurements, Appl. Opt., 27(15), 3250–3254, 1988.

Del Bianco, S., Carli, B., Cecchi-Pestellini, C., Dinelli, B. M., Gai, M., and Santurri, L.: Retrieval of minor constituents in a cloudy atmosphere with remote-sensing millimetre-wave measurements., Q. J. Roy. Meteor. Soc., 133(S2), 163–170, 2007.

Dinelli, B. M., Alpaslan, D., Carlotti, M., Magnani, L., and Ridolfi, M.: Multi-target retrieval (MTR): The simultaneous retrieval of pressure, temperature and volume mixing ratio profiles from limb-scanning atmospheric measurements., J. Quant. Spectrosc. Radiat. Transfer, 84(2), 141–157, 2004.

Dinelli, B. M., Baronti, S., Bazzini, G., Blom, C., Carli, B., Castelli, E., Ceccherini, S., Cecchi Pestellini, C., Chipperfield, M., Cortesi, U., Del Bianco, S., Dudhia, A., Flaud, J. M., Gai, M., Magnani, L., Piccolo, C., Raspollini, P., Ridolfi, M., Santurri, L., and Urban, J.: The Scientific Analysis of Limb Sounding Observations of the Upper Troposphere, Final Report of ESA ESTEC/Contract 16530/02/NL/MM, 2007.

Ekström, M., Eriksson, P., Rydberg, B., and Murtagh, D. P.: First Odin sub-mm retrievals in the tropical upper troposphere: humidity and cloud ice signals, Atmos. Chem. Phys., 7, 459–469, 2007.

Ekström, M., Eriksson, P., Read, W. G. et al.: Comparison of satellite limb-sounding humidity climatologies of the uppermost tropical troposphere, Atmos. Chem. Phys., 8, 309–320, 2008.

Eriksson, P., Ekström, M., Rydberg, B., et al.: First Odin sub-mm retrievals in the tropical upper troposphere: ice cloud properties, Atmos. Chem. Phys., 7, 471–483, 2007.

Eriksson, P., Ekström, M., Rydberg, B., et al.: Comparison between early Odin-SMR, Aura MLS and CloudSat retrievals of cloud ice mass in the upper tropical troposphere, Atmos. Chem. Phys., 8, 1937–1948, 2008.

Fueglistaler, S., Wernli, H., and Peter, T.: Tropical Troposphere-to-Stratosphere Transport Inferred from Trajectory Calculations, J. Geophys. Res., 109, D03108, doi:10.1029/2004JD005516, 2004.

Froidevaux, L., Livesey, N. J., Read, W. G., Jiang, Y. B. Jimenez, C. J., Filipiak, M. J., Schwartz, M. J., Santee, M. L., Pumphrey, H. C., Jiang, J. H., Wu, D. L., Manney, G. L., Drouin, B. J., Waters, J.W., Fetzer, E.J., Bernath, P. F., Boone, C. D., Walker, K. A., Jucks, K. W., Toon, G. C., and Margitan, J. J.: Early validation analyses of atmospheric profiles from EOS MLS on the Aura satellite, IEEE T. Geosci. Remote Sens., 44, 1106–1121, 2006.

Hartmann, G. K., Bevilacqua, R. M., Schwartz, P. R., Kiimpfer, N., Kunzi, K. F., Aellig, C. P., Berg, A., Boogaerts, W., Connor, B. J., Croskey, C. L., Daehler, M., Degenhardt, W., Dieken, H. D., Goldizena, D., Kriebel, D., Langen, J., Loidl, A., Oliveros, J. J., Pauls, T. A., Puliafito, S. E., Richards, M. L., Rudin, C., Tsou, J. J., Waltman, W. B., Umlauft, G., and Zwick, R.: Measurements of O_3, H_2O and ClO in the middle atmosphere using the millimeter-wave atmospheric sounder (MAS), Geophys. Res. Lett., 23, 2313–2316, 1996.

Holton, J. R., Haynes, P. H., Douglass, A. R., Rood, R. B., and Pfister, L.: Stratosphere-troposphere exchange, Rev. Geophys., 33, 403–439, 1995.

IPCC Climate Change 2007: The Physical Science Basis. Contribution of Working Group I to the Fourth Assessment Report of the IPCC, 2007.

Keim, C., Blom, C. E.; von der Gathen, P., Gulde, T., Höpfner, M., Liu, G. Y., Oulanovski, A., Piesch, C., Ravegnani, F., Sartorius, C., Schlager, H., and Volk, C. M.: Validation of MIPAS-ENVISAT by correlative measurements of MIPAS-STR. Proc.

ACVE-2 meeting, 3–7 May 2004, Frascati, Italy, ESA SP-562, 2004.

Kelder, H., van Weele, M., Goede, A., Kerridge, B., Reburn, J., Bovensmann, H., Monks, P., Remedios, J., Mager, R., Sassier, H., and Baillon, Y.: Operational Atmospheric Chemistry Monitoring Missions – CAPACITY: Composition of the Atmosphere: Progress to Applications in the user CommunITY, Final Report of ESA contract no. 17237/03/NL/GS, 2005.

Kerridge, B. J., Siddans, R., Reburn, W. J., et al.: Consideration of Mission Studying Chemistry in the UTLS, Final Report, ESTEC Contract No 15457/01/NL/MM, 2004.

Kerridge, B. J., Siddans, R., Reburn, W. J., et al.: Definition of Mission Objectives and Observational Requirements for an Atmospheric Chemistry Explorer Mission Study 2nd Extension, Final Report, ESA Contract 13048/98/NL/GD, CCN4, 2004.

Livesey, N. J., Read, W. G., Froidevaux, L., Waters, J. W., Santee, M. L., Pumphrey, H. C., Wu, D. L., Shippony, Z., and Jarnot, R. F.: The UARS Microwave Limb Sounder version 5 data set: Theory, characterization, and validation, J. Geophys. Res., 108(D13), 4378, doi:10.1029/2002JD002273, 2003.

Masuko, H., Manabe, T., Seta, M., Kasai, Y., Ochiai, S., Irimajiri, Y., Inatani, J, Ikeda, N., Nishibori, T., Ozeki, H., Sato, R., Fujii, Y., Nakajima, T., Watanabe, H., Kikuchi, K., and Koyama, M.: Superconducting Submillimetre-wave Limb Emission Sounder (SMILES) onboard Japanese Experimental Module (JEM) of International SpaceStation (ISS). Geoscience and Remote Sensing Symposium, Proceedings, IGARSS 2000, IEEE 2000 International, 1, 71–73, 2000.

Moyna, B. P., Oldfield, M. L., Goizel, A. S., Gerber, D., Siddans, R., Reburn, W. J., Matheson, D. N., Kerridge, B. J., de Maagt, P. J. I., Langen, J., and Klein, U.: MARSCHALS: airborne simulator of a future space instrument to observe millimetre-wave limb emission from the upper troposphere and lower stratosphere, In SPIE European Remote Sensing Conference, Stockholm, September 2006, 6361, 63610B, 2006.

Murtagh, D., Frisk, U., Merino, F., Ridal, M., Jonsson, A., Stegman, J., et al.: An overview of the Odin atmospheric mission, Can. J. Phys., 80(4), 309–319, 2002.

Oldfield, M., Moyna, B., Allouis, E., Brunt, R., Cortesi, U., Ellison, B., et al.: MARSCHALS: development of an airborne millimetre wave limb sounder, SPIE, 4540, 221–228, 2001.

Reburn, W. J., Siddans, R., Kerridge, B. J., Buhler, S., von Engeln, A., Kunzi, K., et al.: Study on upper troposphere/lower stratosphere sounding, Technical Report, European Space Agency (ESA), ESTEC, 1998.

Remedios, J. J.: Extreme Atmospheric Constituent Profiles for MIPAS, Proceedings, ESTEC, The Netherlands, 20–22 January, 2, 779–783, 1999.

Rodgers, C. D.: Information content and optimization of high spectral resolution remote measurements, Adv. Space Res. 21, 361–367, 1998

Rodgers, C. D.: Inverse Methods for Atmospheric Sounding: Theory and Practice, World Scientific, Singapore, New Jersey, London, Hong Kong, 2000.

Sandor, B. J., Read, W. G., Waters, J. W., Rosenlof, K. H.: Seasonal behavior of tropical to midlatitude upper tropospheric water vapor from UARS MLS, J. Geophys. Res., 103, 25935–25947, 1998.

Spang, R., Remedios, J. J., and Barkley, M. P.: Colour indices for the detection and differentiation of cloud types in infra-red limb emission spectra, Adv. Space Res., 33, 1041–1047, 2004.

Turquety, S., Hadji-Lazaro, J., Clerbaux, C., Hauglustaine, D. A., Clough, T., Cassé, V., Schlüssel, P., and Mégie, G.: Operational trace gas retrieval algorithm for the Infrared Atmospheric Sounder Interferometer, J. Geophys. Res., 109, D21301, doi:10.1029/2004JD00482, 2004.

Vaughan, G., Schiller, C., MacKenzie, A. R., Bower, K., Peter, T., Schlager, H., Harris, N. R. P., and May, P. T.: SCOUT-O3/ACTIVE: High-altitude aircraft measurements around deep tropical convection, B. Am. Meteor. Soc., accepted for publication, 2007. [redacted]**update?**

Wang, P.-H., Minnis, P., McCormack, M. P., Kent, G. S., and Skeens, K. M.: A 6-year climatology of cloud occurrence frequency form Stratospheric Aerosol and Gas Experiment II observations (1985-1990), J. Geophys. Res., 101, 29407–29429, 1996.

Warren, S. G.: Optical constants of ice from the ultraviolet to the microwave, Appl. Opt., 23, 1206–1225, 1984.

Waters, J. W., Froidevaux, L., Harwood, R. S., Jarnot, R. F., Pickett, H. M., Read, W. G., Siegel, P. H., Cofield, R. E., Filipiak, M. J., Flower, D. A., Holden, J. R., Lau, G. K., Livesey, N. J., Manney, G. L., Pumphrey, H. C., Santee, M. L., Wu, D. L., Cuddy, D. T., Lay, R. R., Loo, M. S., Perun, V. S., Schwartz, M. J., Stek, P. C., Thurstans, R. P., Boyles, M. A., Chandra, S., Chavez, M. C., Chen, G.-S., Chudasama, B. V., Dodge, R., Fuller, R. A., Girard, M. A., Jiang, J. H., Jiang, Y., Knosp, B. W., LaBelle, R. C., Lee, K. A., Miller, D., Oswald, J. E., Patel, N. C., Pukala, D. M., Quintero, O., Scaff, D. M., Snyder, W. V., Tope, M. C., Wagner, P. A., and Walch, M. J.: The Earth Observing System Microwave Limb Sounder (EOS MLS) on the Aura satellite, IEEE Transactions on Geoscience and Remote Sensing, 44(5), 1075–1092, 2006.

Winker, D. M. and Trepte, C. R.: Laminar cirrus observed near the tropical tropopause by LITE, Geophys. Res. Lett., 25, 3351–3354, 1998.

Urban, J., Lautie, N., Le Flochmoen, E., et al.: Odin/SMR limb observations of stratospheric trace gases: Level 2 processing of ClO, N_2O, HNO_3, and O_3, J. Geophys. Res., 110, D14307, doi:10.1029/2004JD005741, 2005.